

EFFECT OF CLAY SHALE SHEAR STRENGTH DEGRADATION ON BORED PILE FRICTION IN CLAY SHALE

Rifqi B Arief^a, Masyhur Irsyam^a, Idrus M Alatas^b, Sugeng Krisnanto^a, Endra Susila^a, Hasbullah Nawir^a, Ramli Nazir^c

^aCivil Engineering Program, Bandung Institute of Technology, Bandung, Indonesia

^bCivil Engineering Department, National Institute of Science and Technology, Jakarta, Indonesia

^cSchool of Civil Engineering, Universiti Teknologi Malaysia, 81310 UTM Johor Bahru, Johor, Malaysia

Article history

Received

20 January 2022

Received in revised form

4 July 2022

Accepted

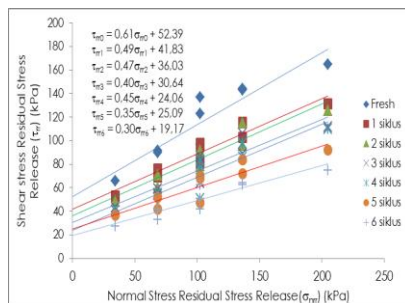
5 July 2022

Published Online

21 August 2022

*Corresponding author
rifqi2016@students.itb.ac.id

Graphical abstract



Abstract

This research aims at investigating and modeling the axial bearing capacity degradation of a bored pile on clay shale due to the bored pile installation processes. Clay shale sample models were prepared to simulate the wetting and drying cycles through weathering process between 0 to 6 hours. All samples were tested in which every 1 hour of the weathering process representing 1 cycle of wetting and drying. The direct shear laboratory tests were performed to obtain the peak and residual shear strength parameters of the interface between the bored pile and clay shale. The peak and residual shear strength parameters were obtained after 6 hours of the weathering process. The residual shear strength parameters were measured by applying with and without stress release. This investigation showed that the shear strength degradation at peak, residual without stress release, and residual with stress release respectively reached 87-62%, 28-20%, and 25-14% after 1 to 6 hours of weathering process. This result is very useful for predicting the bored pile skin friction in clay shale soils.

Keywords: Clay shale, bored pile friction, shear strength degradation, weathering, direct shear

Abstrak

Penyelidikan ini bertujuan untuk menyiasat dan memodelkan kemerosotan kapasiti galas paksi cerucuk bored pada syal tanah liat akibat proses pemasangan cerucuk bored. Model sampel syal tanah liat telah disediakan untuk mensimulasikan kitaran pembasahan dan pengeringan melalui proses luluhawa antara 0 hingga 6 jam. Semua sampel telah diuji di mana setiap 1 jam proses luluhawa mewakili 1 kitaran pembasahan dan pengeringan. Ujian makmal ricih langsung telah dilakukan untuk mendapatkan parameter kekuatan ricih puncak dan baki antara muka antara cerucuk greek dan syal tanah liat. Parameter kekuatan ricih puncak dan baki diperoleh selepas 6 jam proses luluhawa. Parameter kekuatan ricih sisa diukur dengan menggunakan dengan dan tanpa pelepasan tegasan. Penyiasatan ini menunjukkan bahawa kemerosotan kekuatan ricih pada puncak, baki tanpa pelepasan tegasan, dan baki dengan pelepasan tegasan masing-masing mencapai 87-62%, 28-20%, dan 25-14% selepas 1 hingga 6 jam proses luluhawa. Keputusan ini sangat berguna untuk meramalkan geseran kulit cerucuk bosan dalam tanah syal tanah liat.

Kata kunci: Syal tanah liat, geseran cerucuk bored, degradasi kekuatan ricih, luluhawa, ricih langsung

© 2022 Penerbit UTM Press. All rights reserved

1.0 INTRODUCTION

Previous investigation indicates that several problems will occur when excavation is conducted for bored pile installation in clay shale [1] that result in the reduction of bored pile friction resistance. Drilling time up to casting concrete that is more than 2 hours can cause significant friction resistance degradation. The small-scale bored hole in clay shale for bored piles has been conducted before in a laboratory by Labiouse and Vietor [2]. The clay shale bored hole commonly has a microfracture parallel to the bedding plane on two sides of the bored hole. The hole side is parallel to the bedding plane moving to the hole, and then the bored hole narrows [3], as shown in Figure 1. It shows time-dependent fracture formation. Other study [4] also shows that the fracture parallel to the bedding plane curved into the bored hole. A numerical study [5] confirmed that the fracture around the bored hole was occurred due to the time-dependent excavation

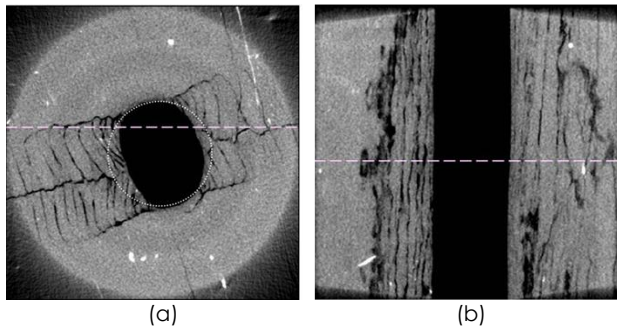


Figure 1 X-ray computed tomography scan of the central part of the Opalinus Clay hollow cylinder specimen[2] (a) cross section (b) inside the hole

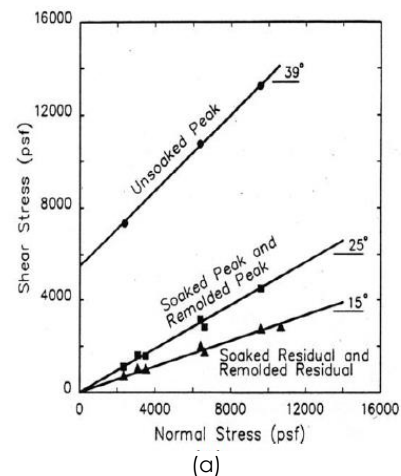
The level clay shale shear strength degradation used to calculate the bearing capacity of the bored pile in each location is different due to mineral contents [7] and depends on the length of drilling time [1]. The degradation of bored pile friction resistance in clay shale occurs as clay shale shear strength is degraded. If clay shale is exposed to sunlight, air, and water in a short time, it will slake and change into soft clay [7]. The previous studies mentioned that clay shale is an integral part of claystone (Clay-Bearing Rocks) [8], mudstone, and siltstone [9]. Those changes can be in the form of physical disintegration or chemical decomposition. In tropical climate areas, such as Indonesia, the process is generally more common than other climatic conditions [10]. In general, the claystone mineralogy is mainly composed of fine-grained particles, i.e., clay minerals. It is widely known that the rocks containing Smectite and Pyrite minerals may be damaged when exposed to air and water [11]. From the drained direct shear test, the shear strength of the soaked clay shale dramatically decreased compared to the unsoaked clay shale. The soaked and remoulded residual shear strength will be lower

[12] when compared to the soaked and remoulded peak stress as shown in Figure 2(a) [13]. The weathering effects have been studied [14] as shown in Figure 2(b).

Alatas [15] has conducted a study to figure out the clay shale shear strength degradation by drying and wetting the clay shale in 80 days. The shear strength was measured using a multi-stage triaxial Test. The frequently wetting and drying phenomena could create a rapid weathering process. The results showed clay shale shear strength degradation at peak, residual, and stress release (RTS) conditions as shown in Figure 3. The cohesion and angle of internal friction decreased in all stress conditions. Unconfined compression test on Pamplona marl clay shale soaked for 5 minutes caused the peak shear strength of clay shale to decrease by 8% [16].

Friction between two different material surfaces had been investigated using standard and modified direct shear tests [17]. The Tests to find the value of clay shale skin friction using direct shear between concrete and calcarenite rock have been conducted to figure out the effect of the roughness of bored hole walls [17], soil – cement of soil nailing [18], shale, and casing [19], soil – concrete of bored pile [20].

This research proposed several equations describing the relationship between the adhesion factor of bored pile in clay shale and peak clay shale shear strength. These adhesion factors resulted from a laboratory study simulating the clay shale shear strength degradation due to excavation. The work presented in this paper is also a continuation from the study conducted by Alatas [6] on time-dependent degradation of clay shale shear strength utilizing triaxial yet focused on the bored pile friction.



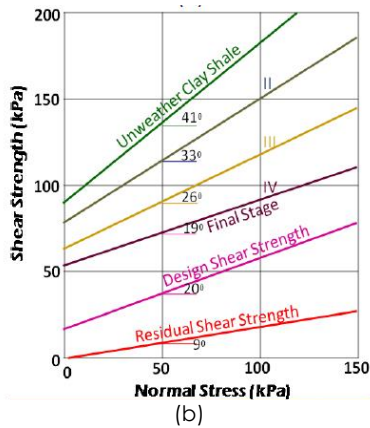


Figure 2 Results of (a) clay shale shear strength degradation from peak and residual with unsoaked and soaked samples [10] and (b) degradation of clay shale shear strength due to weathering effect [11]

2.0 METHODOLOGY

In this study, the friction resistance of a bored pile in clay shale was modeled in a laboratory using direct shear test. The excavation-weathered clay shale was also simulated using cycles of wetting and drying. Disturbed and undisturbed samples were gathered from the Semarang-Bawen Highway at STA 438. The undisturbed samples were collected using a core drill to generate accurate shear strength parameters. The core drill bit had the same diameter as the direct shear split box pit, which was 60.5 mm. The samples were obtained using a core drill shown in Figure 4 and were properly sealed in black plastic (which was not exposed to sunlight and water) as well as put in a pipe to prevent from collision.

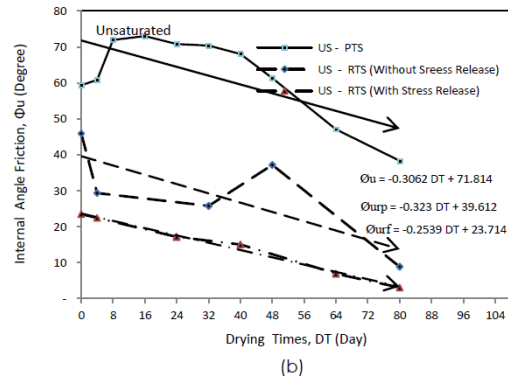


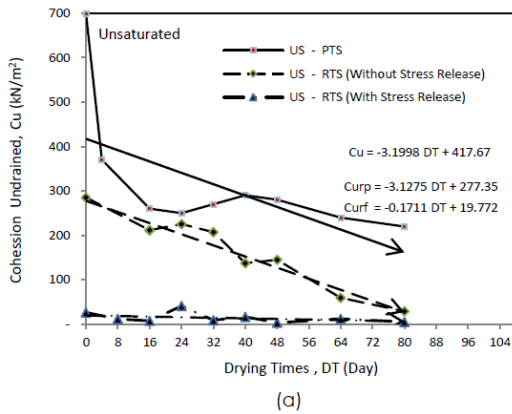
Figure 3 Results of (a) cohesion degradation and (b) internal angle friction degradation up to 80 days of drying process for saturated clay shale samples at Peak Total Stress (S-PTS) and Residual Total Stress (S-RTS)[15]

The initial shear strength of clay shale $\phi = 59.4^\circ$ and $c = 700 \text{ kN/m}^2$ [15] were used to measure the shear strength degradation. Clay shale surrounding the bored pit was modeled to be exposed to light, air, and submerged. When drilling with water, the excavated area was exposed to air and sunlight. This process was conducted at 0 hour, 1 hour, 2 hours, 3 hours, 4 hours, 5 hours, and 6 hours because the shear strength of clay shale would be degraded by the bored pile installation which took more than 2 hours [1]. Therefore, the modeling is adequate up to 6 hours. Each sample was submerged for 5 minutes as the water in bored pit during excavation. To simulate the circumstance of clay shale in a drilled pile pit, which is not exposed to direct sunlight, the draining process was carried out in a room condition with no direct sunlight.

In this test, clay shale samples were put in the bottom split box and wet concrete in the upper split box as shown in Figure 5. Then, a 3-day curing process is carried out on the direct shear sample, to ensure the setting process of the concrete layer. Each sample was subjected to different normal stresses in the laboratory. The normal stress was measured from the lateral stress on the bored pile at the Lemah Ireng Bridge nearby to the sampling location.

The test was proceeded using a multi-stage direct shear. Each sample was sheared until it reached its peak strength and decreased to the residual strength. Then, normal stress was added to the same sample and sheared until it reached its peak strength. This process was repeated twice. In order to obtain the residual shear strength stress release condition, the normal stress was removed from the sample and proceeded with the multi-stage reversal direct shear as shown in Figure 6. This process was carried out using the same procedure as multi-stage direct shear but in the reverse direction.

Figure 7 shows the experimental stages which was used in the analysis. The normal stress for the first sheared sample was 34 kN/m^2 (NP-1), after it reaches its residual shear strength, then the normal stress was



increased to 68 kN/m² (NP-2), and finally to 103 kN/m² (NP-3). At last, the normal stress level was set to zero and followed by the multi-stage reversal direct shear.

The initial normal stresses for the second sample were 68.3 kN/m² (NP-2), 103 kN/m² (NP-3), and 137 kN/m² (NP-4). Meanwhile, the initial normal stresses for the third sample were 103 kN/m² (NP-3), 137 kN/m² (NP-4), and 205 kN/m² (NP-5). These normal stresses then were used for the next 6 cycles.



Figure 4 Taking samples using a core drill

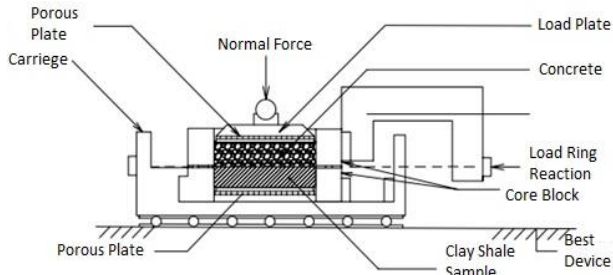


Figure 5 Placement of clay shale and concrete for direct shear test

3.0 RESULTS AND DISCUSSION

The values of peak shear stress (τ) were plotted with normal stress (σ_n) to describe peak shear strength in each cycle as shown in Figure 8. The values of residual shear stress were shown in Figure 9, while those of stress release was shown in Figure 10.

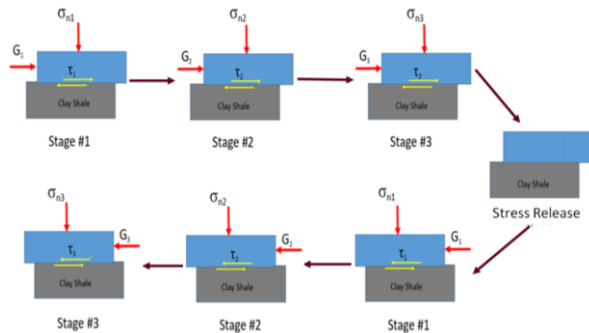


Figure 6 Multistage reversal mechanisms in direct shear testing

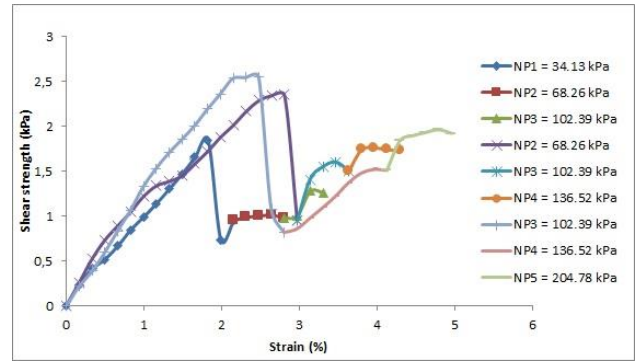


Figure 7 Normal stress applied to each sample in multi-stage direct shear testing

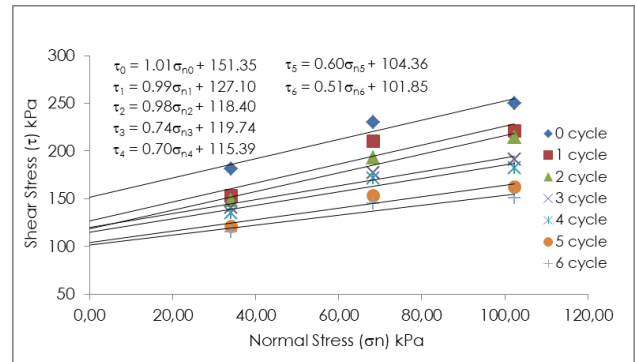


Figure 8 Shear stress (τ) vs normal stress (σ_n) at peak stress from the test results.

The lines connecting points in Figures 8, 9, and 10 were deduced using linear regressions. The linear regressions produced adhesion (a_c) and interface friction angle (δ). The direct shear test results show that peak friction angle was between 45.3° and 27°, while peak adhesion (a_c) was between 151.4 kPa and 101.9 kPa. The results also show that residual strength of the friction angle (δ) was between 36.9° and 20.8°, while residual strength of adhesion (a_c) was between 49.4 kPa and 32.4 kPa. The residual strength stress release condition of friction angle (δ) was between 31.4° and 16.2°, whereas that of adhesion (a_c) was between 52.4 kPa and 19.2 kPa.

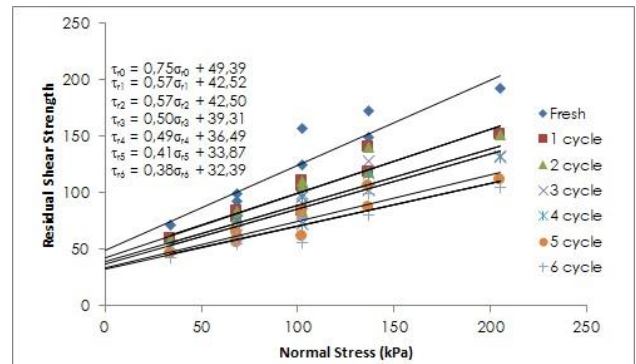


Figure 9 Shear stress (τ_r) vs. normal stress (σ_{nr}) at the residual stress from the test results

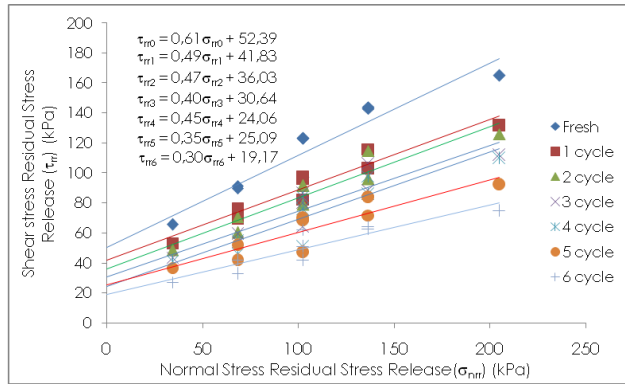


Figure 10 Shear stress (τ_{rr}) vs. normal stress (σ_{nr}) at the residual stress with stress release from the test results

In each cycle, the interface shear strength parameters of the bored pile and clay shales, such as adhesion (a_c) as well as friction angle of clay shale and bored pile (δ) can be calculated (see Figures 8, 9, and 10). The regression results of each parameter then were plotted in Figures 11 and 12. These figures show that the adhesion (a_c) and interface friction angle between the concrete and clay shale (δ) from the peak stress was greater than those of residual stress and residual stress release conditions. At the same time, the shear strength at the residual stress condition were almost the same as those at residual stress release.

To quantify the shear strength degradation, the ratio of shear stress (τ) and normal stress (σ_n) were calculated. Therefore, the shear strength degradation was not affected by depth and normal stresses. To determine the clay shale shear strength degradation without normal stress dependence, the stress ratio in each peak, residual without stress release, and residual with stress release condition were calculated. The shear strength degradations for each stress condition are shown in Figure 13.

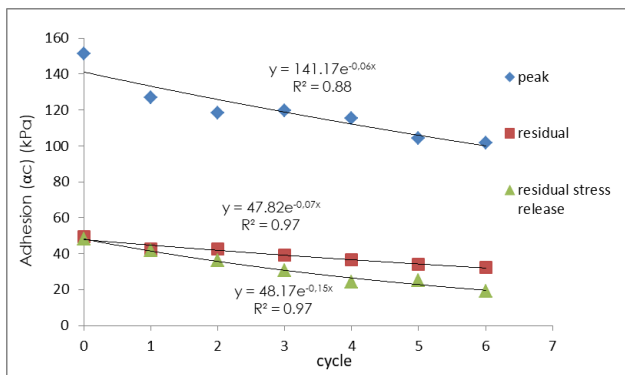


Figure 11 Pile and clay shale adhesion degradation at peak, residual, and stress release conditions per cycle

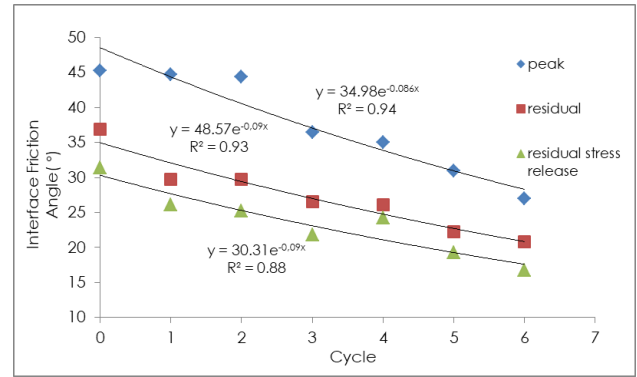


Figure 12 Degradation pile and clay shale interface friction angle at peak, residual, and stress release vs. cycle

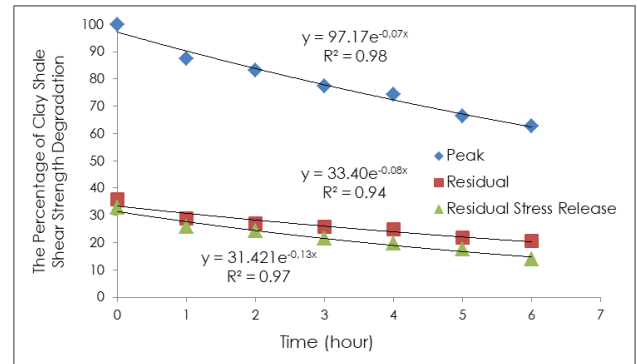


Figure 13 Clay shale shear degradation at peak, residual, and stress release condition vs. time (hour)

In this study, the reduction coefficient (β) was defined as the ratio of soil-pile friction to the initial internal friction angle of clay shale ($\beta = \tan \delta / \tan \phi$) as shown in Table 1, Figure 14, and Figure 15 for peak, residual, and stress release. Meanwhile, the adhesion factor (α) was calculated by dividing adhesion (a_c) by cohesion (c) as shown in Table 2, Figure 16, and Figure 17.

Table 1 Soil-pile friction angle and internal friction angle at each peak, residual, and stress release condition

Peak		Residual		Stress Release	
δ	β	δ_r	β_r	δ_{rr}	β_{rr}
45.29	0.76	36.87	0.62	31.38	0.53
44.71	0.75	29.68	0.76	26.10	0.44
44.42	0.75	29.68	0.72	25.17	0.42
36.50	0.61	26.57	0.71	21.80	0.37
34.99	0.59	26.10	0.63	24.23	0.41
30.96	0.52	22.29	0.55	19.29	0.32
27.02	0.45	20.81	0.53	16.70	0.28

Table 2 Soil-pile skin resistances and cohesions at each peak, residual, and stress release condition

Peak		Residual		Stress Release	
Ac	c	Ac	c _r	Ac	c _{rr}
151.35	0.22	49.00	0,07	52,39	0,07
127.10	0.18	43.00	0,06	41.83	0,06
118.40	0.17	36.00	0,05	36,03	0,05
119.74	0.17	39.00	0,05	30,64	0,04
115.39	0.16	36.00	0,05	24.06	0,03
104.36	0.15	34.00	0,05	25.09	0,03
101.85	0.15	32.00	0,04	19.17	0,03

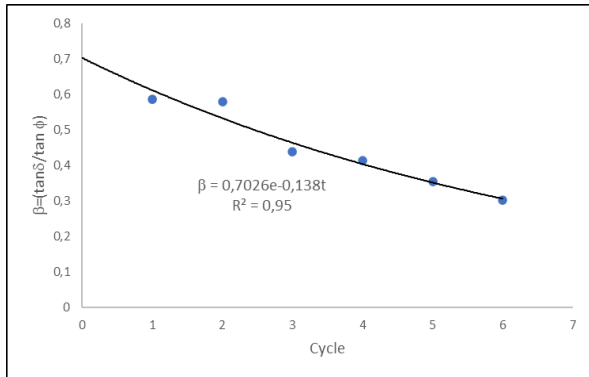


Figure 14 Reduction coefficients in peak condition vs. cycle

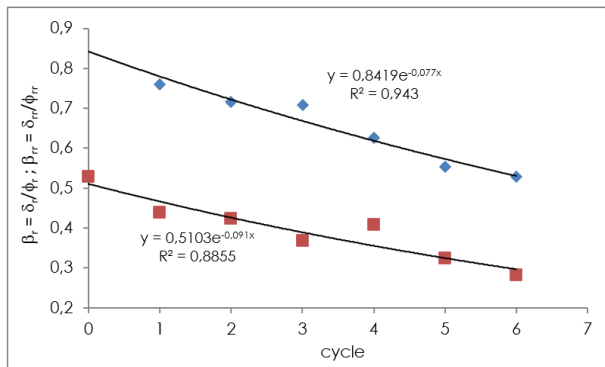


Figure 15 Reduction coefficients in residual and stress release vs. cycle

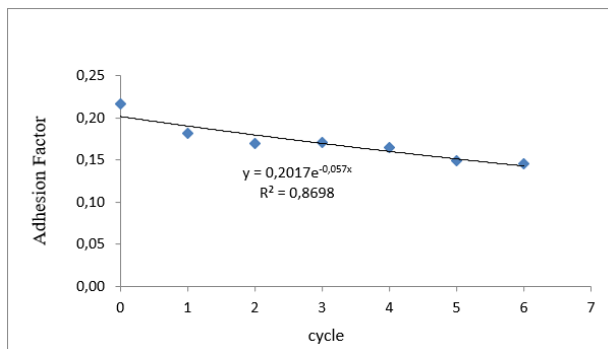


Figure 16 Adhesion factors in peak condition vs. cycles

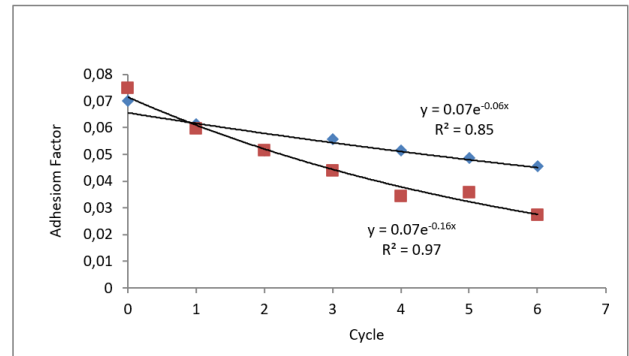


Figure 17 Adhesion factors in residual stress and stress release vs. cycles

4.0 CONCLUSION

The results of the laboratory tests show that the interface shear strength was greatly degraded when clay shale samples were exposed to air, light, and wetting. The effect of wetting of the clay shale in a room for up to 6 cycles (1 hour for each cycle) led to the degradation of both peak and residual shear strengths. The shear strength parameters decreased as weathering time increased. The initial adhesion of clay shale, with and without stress release, significantly decreased after 6 hours. After 6 hours of simulated weathering, the shear strength degradation in peak and residual conditions was achieved. The residual shear strength parameters were separated based on whether the residual shear strength was with or without stress release.

This investigation showed that the shear strength degradation at peak, residual without stress release, and residual with stress release respectively reached 87-62%, 28-20%, and 25-14% after 1 to 6 hours of weathering process. This result can be used for predicting the bored pile skin friction in clay shale soils.

Moreover, in this study, the adhesion factor (a) was measured using the average adhesion factor per cycle in each condition. The adhesion factor (a) for peak stress, residual stress, and stress release conditions was 0.17, 0.06, and 0.05, respectively. In this study, the determination adhesion factor was derived from the average of a per cycle in each condition. The reduction factor (beta) for peak stress, residual stress, and stress release conditions was 0.63, 0.46, and 0.40, respectively.

Acknowledgement

This research was funded by LPDP (Education Fund Management Institute from Indonesian Ministry of Finance) and Bandung Institute of Technology. The sample was collected with permission of Trans Marga Central Java. Laboratory testing is facilitated by Mr. Idrus M Alatas. The author would like to express his

sincere appreciation to the Civil Engineering Program Bandung Institute of Technology, LPDP, Trans Marga Central Java, and Mr. Idrus M Alatas.

References

- [1] Irsyam, M., Sahadewa, A., Boesono, A., and Soebagyo. 2007. Pengaruh Strength Reduction Tanah Clay-Shale Akibat Pelaksanaan Pemboran Terhadap Nilai Daya Dukung Pondasi Tiang di Jembatan Suramadu Berdasarkan Analisis Hasil Tes OC. *Jurnal Teknik Sipil*. 14(2): 69-82.
DOI: 10.5614/jts.2007.14.2.1.
- [2] Labiouse V. and Vietor T. 2014. Laboratory and In Situ Simulation Tests of the Excavation Damaged Zone Around Galleries in Opalinus Clay. *Rock Mechanics and Rock Engineering*. 47: 57-70.
DOI: 10.1007/s00603-013-0389-4.
- [3] Kupferschmied, N., Wild, K. M., Amann, F., Nussbaum, C., Jaeggi, D., and Badertscher, N. 2015. Time-dependent Fracture Formation Around a Borehole in a Clay Shale. *International Journal of Rock Mechanics & Mining Sciences*. 77: 105-114.
DOI: 10.1016/j.ijrmms.2015.03.027.
- [4] Pašić, B., Međimurec, N.G, Matanović, D. 2007. WELLBORE INSTABILITY: Causes and Consequences Nestabilnost Kanala Bušotine: Uzroci I Posljedice. *Rudarsko-Geološko-Naftni Zbornik*. 19: 87-98.
- [5] Lisjak, A., Grasselli, G., and Vietor, T. 2014. Continuum-Discontinuum Analysis of Failure Mechanisms Around Unsupported Circular Excavations in Anisotropic Clay Shales. *International Journal of Rock Mechanics & Mining Sciences*. 65: 99-115.
DOI: 10.1016/j.ijrmms.2013.10.006.
- [6] Alatas, I. M., Kamaruddin, S. A., Nazir, R., and Irsyam, M. 2016. Effect of Weathering on Disintegration and Shear Strength Reduction of Clay Shale. *Jurnal Teknologi*. 78: 7-3.
DOI: 10.11113/jt.v78.9491.
- [7] Shakir, R. R., Zhu, J-G. 2010. An Examination of the Mechanical Interaction of Drilling Slurries at the Soil-concrete Contact. *Applied Physics & Engineering*. 11(4): 294-304
- [8] Shakoor, A., Tej. P. G. 2011. Slaking Behavior of Clay-Bearing Rocks during a One-year Exposure to Natural Climatic Conditions. *Engineering Geology*. 166:17-25.
DOI: 10.1016/j.enggeo.2013.08.003.
- [9] Nandi, A. and Shakoor, A. 2008. Application of Logistic Regression Model for Slope Instability Prediction in Cuyahoga River Watershed, Ohio, USA. *Georisk*. 2(1): 16-27.
DOI: 10.1080/17499510701842221.
- [10] Sadisun, I. A., Bandonu, Shimada, H., Ichinose, M., and Matsui, K. 2010. Physical Disintegration Characterization of Mudrocks Subjected to Slaking Exposure and Immersion Tests. *Jurnal Geologi Indonesia*. 5(4): 219-225.
DOI: 10.17014/ijog.v5i4.105.
- [11] Sadisun, I. A., Bandonu, H., Shimada, M., Ichinose, and Matsui, K. 2004. Textural and Mineralogical Properties of Argillaceous Rocks in Relation to Their Propensity to Slaking. *4th Asian Symposium on Engineering Geology and the Environment: Engineering Geology for Sustainable Development at Mountainous Areas*.
DOI: 10.13140/2.1.2287.4248.
- [12] Widjaya, B. 2008. Engineering Characteristics of Bukit Sentul Clayshale based on Laboratory and In Situ Tests. *Proceeding of Conference: International Site Characterization (ISC) 3A: Taipei, Taiwan*. 1231-1237.
DOI: 10.13140/RG.2.1.2559.3445
- [13] Timothy, D. S., Duncan, and Michael. 1991. Mechanisms of Strength Loss in Stiff Clays. *Journal of Geotechnical Engineering*. 117(1): 139-154.
DOI: 10.1061/(ASCE)0733-9410(1991)117:1(139).
- [14] Gartung, E. 1986. Excavation of the Hard Clays of the Keuper Formation. *Proceeding of Symposium Geotechnical Engineering Division*. Seattle, Washington.
DOI:10.1016/0148-9062(87)92601-5.
- [15] Alatas, I. M., Kamaruddin, S. A., Nazir, R., and Irsyam, M. 2015. Shear Strength Degradation of Semarang Bawen Clay Shale Due to Weathering Process. *Jurnal Teknologi*. 77: 109-118.
DOI: 10.11113/jt.v77.6429.
- [16] Alonso, E. E., Pineda, J. A. 2006, Weathering and Degradation of Shales: Experimental Observations and Models of Degradation. *Conference: VI South American Rock Mechanics Conference at: Cartagena de Indias, Colombia*. 249-296.
- [17] Johnston, I. W., Novello, E. A., Carter, J. P., Ooi, L. H. 1988. Constant Normal Stiffnes Direct Shear Testing of Calcarenite. *International Conference Engineering For Calcareous Sediments*. 541-553.
DOI: 10.1520/GTJ10132J.
- [18] Pellet, F. L., Keshavarz, M. 2014. Shear Behavior of the Interface between Drilling Equipments and Shale Rocks. *Journal Petrol Exploration Production Technolgy*. 4: 245-254.
DOI 10.1007/s13202-014-0108-z.
- [19] Chu, L. M., Yin, J. H. 2007. Study on Soil-cement Grout Interface Shear Strength of Soil Nailing by Direct Shear Box Testing Method. *Geomechanics and Geoengineering: An International Journal*. 1(4): 259-273.
DOI: 10.1080/17486020601091742.
- [20] Haeri, H., Fatehimarji, M. 2009, Investigation of Shear Behavior of Soil-concrete Interface. *Smart Structures and Systems*. 23(1): 81-90.
DOI: 10.12989/sss.2019.23.1.081.